Analysis and optimization of the thermal performance of microchannel heat sinks

Dong Liu and Suresh V. Garimella
Cooling Technologies Research Center, School of Mechanical Engineering, Purdue University, West Lafayette, Indiana, USA

Received February 2003
Revised November 2003
Accepted May 2004

Abstract

Purpose – To provide modeling approaches of increasing levels of complexity for the analysis of convective heat transfer in microchannels which offer adequate descriptions of the thermal performance, while allowing easier manipulation of microchannel geometries for the purpose of design optimization of microchannel heat sinks.

Design/methodology/approach – A detailed computational fluid dynamics model is first used to obtain baseline results against which five approximate analytical approaches are compared. These approaches include a 1D resistance model, a fin approach, two fin-liquid coupled models, and a porous medium approach. A modified thermal boundary condition is proposed to correctly characterize the heat flux distribution.

Findings – The results obtained demonstrate that the models developed offer sufficiently accurate predictions for practical designs, while at the same time being quite straightforward to use.

Research limitations/implications – The analysis is based on a single microchannel, while in a practical microchannel heat sink, multiple channels are employed in parallel. Therefore, the optimization should take into account the impact of inlet/outlet headers. Also, a prescribed pumping power may be used as the design constraint, instead of pressure head.

Practical implications – Very useful design methodologies for practical design of microchannel heat sinks.

Originality/value – Closed-form solutions from five analytical models are derived in a format that can be easily implemented in optimization procedures for minimizing the thermal resistance of microchannel heat sinks.

Keywords Optimization techniques, Heat transfer, Convection

Paper type Technical paper

Nomenclature

A_c	=	microchannel cross-sectional area	h	=	heat transfer coefficient
A_f	=	fin cross-sectional area	H	=	height of heat sink
A_s	=	area of heat sink	H_c	=	microchannel depth
C_p	=	specific heat	k	=	thermal conductivity
D_h	=	hydraulic diameter	L	=	length of heat sink
fRe	=	friction constant	$\dot{m}$	=	mass flow rate

The authors acknowledge the financial support from members of the Cooling Technologies Research Center (available at: http://widget.ecn.purdue.edu/~CTRC), a National Science Foundation Industry/University Cooperative Research Center at Purdue University.

International Journal for Numerical Methods in Heat & Fluid Flow
Vol. 15 No. 1, 2005
pp. 7-26

0961-5539
DOI 10.1108/09615530510571921

n = number of microchannels
Nu = Nusselt number
P = pressure
q'' = heat flux
q = heat removal rate
Q = volume flow rate
R = thermal resistance
Re = Reynolds number
t = substrate thickness
T = fin temperature
T_b = temperature at the base of the fin
T_f = fluid temperature
u_m = mean flow velocity
W = width of heat sink
w_c = microchannel width
w_w = fin thickness

Greek symbols
α = aspect ratio of microchannels
η_f = fin efficiency
μ = dynamic viscosity
θ = thermal resistance
ρ = density of fluid
ΔP = pressure drop
ΔT = temperature difference

Subscripts and superscripts
c = channel fluid
f = fluid
i = inlet
s = solid fin
w = wall

Introduction

The potential for handling ultra-high heat fluxes has spurred intensive research into microchannel heat sinks (Tuckerman and Pease, 1981; Weisberg and Bau, 1992; Sobhan and Garimella, 2001). For implementation in practical designs, the convective heat transfer in microchannels must be analyzed in conjunction with the choice and optimization of the heat sink dimensions to ensure the required thermal performance. Design procedures are also needed to minimize the overall thermal resistance.

The focus of this paper is to present a comprehensive discussion and comparison of five different (approximate) analytical models of increasing sophistication, which offer closed-form solutions for single phase convective heat transfer in microchannels. A general computational fluid dynamics (CFD) model is first set-up to obtain an "exact" solution. Details of the approximate models and the assumptions involved are then presented along with a comparison of the thermal resistance predictions from these models. Optimization of the thermal performance of microchannel heat sinks is then discussed.

Description of the problem

The microchannel heat sink under consideration is shown in Figure 1. Materials for fabrication may include conductive materials such as copper and aluminum for modular heat sinks or silicon if the microchannels are to be integrated into the chip. For conservative estimates of thermal performance, the lid (top plate) may be

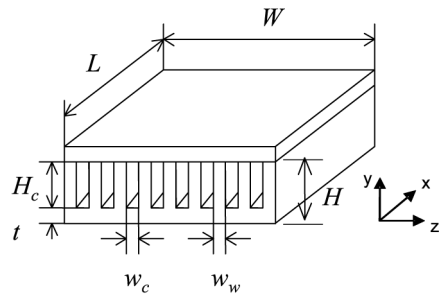

Figure 1.
Schematic of a microchannel heat sink

to be insulated. The width of individual microchannels and intervening fins (w_c+w_w) is typically small compared to the overall heat sink dimension W, and numerous channels are accommodated in parallel flow paths.

Continuum equations for conservation of mass, momentum and energy, respectively, for the convective heat transfer in microchannel heat sinks can be written as (Fedorov and Viskanta, 2000; Toh *et al.*, 2002):

$$\nabla \cdot (\rho \vec{V}) = 0 \tag{1}$$

$$\vec{V} \cdot \nabla(\rho \vec{V}) = -\nabla P + \nabla \cdot (\mu \nabla \vec{V}) \tag{2}$$

$$\vec{V} \cdot \nabla(\rho C_p T) = \nabla \cdot (k_f \nabla T) \quad \text{for the fluid} \tag{3}$$

$$\nabla \cdot (k_s \nabla T_s) = 0 \quad \text{for the fin} \tag{4}$$

This set of equations assumes steady-state conditions for incompressible, laminar flow, with radiation heat transfer neglected. With an appropriate set of boundary conditions, these equations provide a complete description of the conjugate heat transfer problem in microchannels.

CFD model

A numerical model was formulated to solve the three-dimensional heat transfer in microchannels using the commercial CFD software package, FLUENT (Fluent Inc., 1998). The simulation was performed for three different sets of dimensions as listed in Table I. These three cases are chosen to simulate experiments in the literature (Tuckerman and Pease, 1981) that have often been used for validating numerical studies (Weisberg and Bau, 1992; Toh *et al.*, 2002; Ryu *et al.*, 2002).

The computational domain, chosen from symmetry considerations, is shown in Figure 2. The top surface is adiabatic and the left and right sides are designated symmetric boundary conditions. A uniform heat flux is applied at the bottom surface. In the present work, water is used as the working fluid ($\rho = 997\,\text{kg/m}^3$, $C_p = 4,179\,\text{J/kg K}$, $\mu = 0.000855\,\text{kg/ms}$, and $k_f = 0.613\,\text{W/mK}$ evaluated at 27°C), and silicon is used as the heat sink substrate material with $k_s = 148\,\text{W/mK}$.

In the numerical solution, the convective terms were discretized using a first-order upwind scheme for all equations. The entire computational domain was discretized using a $500 \times 60 \times 14$ (x-y-z) grid. To verify the grid independence of

	Case 1	2	3
w_c (μm)	56	55	50
w_w (μm)	44	45	50
H_c (μm)	320	287	302
H (μm)	533	430	458
ΔP (kPa)	103.42	117.21	213.73
q'' (W/cm^2)	181	277	790
R_{exp} (°C/W) (Tuckerman and Pease, 1981)	0.110	0.113	0.090
R_{num} (°C/W)	0.115	0.114	0.093

Note: $L = W = 1\,\text{cm}$

Table I.
Comparison of thermal resistances

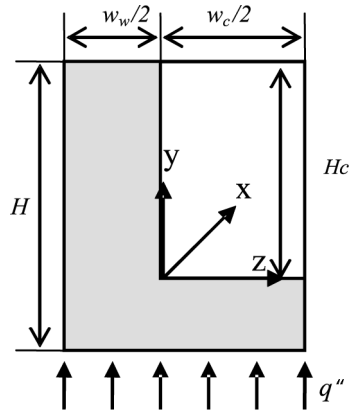

Figure 2.
Computational domain

the convective heat transfer results, three different meshes were used in the fluid part of the domain: 20×5, 30×7, and 50×15. The thermal resistance changed by 3.4 percent from the first to the second mesh, and only by 0.3 percent upon further refinement to the third grid. Hence 30×7 grids were used in the fluid domain for the results in this work.

The agreement between the experimental and predicted values of thermal resistance in Table I validates the use of the numerical predictions as a baseline against which to compare the approximate approaches considered in this work.

The numerical results may also be used to shed light on the appropriate boundary conditions for the problem under consideration. For instance, it is often assumed in microchannel heat sink analyses that the axial conduction in both the solid fin and fluid may be neglected. Using the numerical results for case 1 as an example, the axial conduction through the fin and fluid were found to account for 0.3 and 0.2 percent of the total heat input at the base of the heat sink, respectively. Thus, the assumption of negligible axial conduction appears valid for heat transfer in the silicon microchannels considered.

Two alternative boundary conditions have been commonly used at the base of the fin in microchannel analyses (Zhao and Lu, 2002; Samalam, 1989; Sabry, 2001):

$$-k_{\mathrm{s}} \left. \frac{\partial T}{\partial_y} \right|_{y=0} = q'' \tag{5}$$

or

$$-k_{\mathrm{s}} \left. \frac{\mathrm{d}T}{\mathrm{d}y} \right|_{y=0} = \frac{w_{\mathrm{c}} + w_{\mathrm{w}}}{w_{\mathrm{w}}} q'' \tag{6}$$

in which equation (5) implies that the imposed heat flows evenly into the fluid via the bottom of the microchannel and into the fin via the base of the fin, while equation (6) implies that all the heat from the base travels up the base of the fin. Clearly, neither of

these two extreme cases represent the actual situation correctly. The computed heat flux in the substrate in the immediate vicinity of the fin base is shown in Figure 3 for case 1. The heat fluxes into the fluid and the fin are 55.5 and 333 W/cm^2, respectively. Hence, the error associated with employing equations (5) and (6) as the boundary condition at the base of the fin would be 50 and 24 percent, respectively. A reasonably accurate alternative for the boundary condition could be developed as follows:

$$q = h\left(\frac{w_c}{2}L\right)(T_b - \overline{T}_f) + h(H_c L)\eta_f(T_b - \overline{T}_f) \tag{7}$$

Hence, the ratio of the heat dissipated through the vertical sides of the fin to that flowing through the bottom surface of the microchannel into the fluid is ${}_2\eta_f H_c/w_c$, or ${}_2\eta_f\alpha$. This leads to a more reasonable boundary condition at the base of the fin:

$$-k_s \left.\frac{dT}{dy}\right|_{y=0} = \frac{2\eta_f\alpha}{2\eta_f\alpha + 1}\frac{w_c + w_w}{w_w}q'' \tag{8}$$

This condition results in a heat flux of 366 W/cm^2 through the base of the fin, which is within 10 percent of the computed exact value of 333 W/cm^2.

In light of this discussion, equation (8) is imposed as the thermal boundary condition at the base of the fin for all the five approximate models developed in this work.

Approximate analytical models

In view of the complexity and computational expense of a full CFD approach for predicting convective heat transfer in microchannel heat sinks, especially in searching for optimal configurations under practical design constraints, simplified modeling approaches are sought. The goal is to account for the important physics, even if some

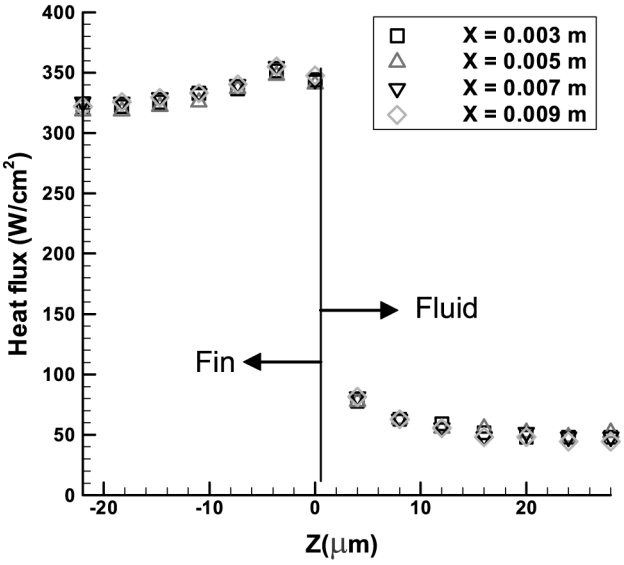

Figure 3.
Heat flux distribution at the base of the fin

of the details may need to be sacrificed. Five approximate analytical models (Zhao and Lu, 2002; Samalam, 1989; Sabry, 2001; Kim and Kim, 1999) are discussed, along with the associated optimization procedures needed to minimize the thermal resistance. The focus in this discussion is on the development of a set of thermal resistance formulae that can be used for comparison between models, as well as for optimization of microchannel heat sinks.

As shown in Figure 1, for the problem under consideration, the fluid flows parallel to the x-axis. The bottom surface of the heat sink is exposed to a constant heat flux. The top surface remains adiabatic.

The overall thermal resistance is defined as:

$$R_o = \frac{\Delta T_{max}}{q'' A_s} \tag{9}$$

where $\Delta T_{max} = (T_{w,o} - T_{f,i})$ is the maximum temperature rise in the heat sink, i.e. the temperature difference between the peak temperature in the heat sink at the outlet ($T_{w,o}$) and the fluid inlet temperature ($T_{f,i}$). Since the thermal resistance due to substrate conduction is simply:

$$R_{cond} = \frac{t}{k_s(LW)} \tag{10}$$

the thermal resistance R calculated in following models will not include this term:

$$R = R_o - R_{cond} \tag{11}$$

The following assumptions are made for the most simplified analysis:

(1) steady-state flow and heat transfer;
(2) incompressible, laminar flow;
(3) negligible radiation heat transfer;
(4) constant fluid properties;
(5) fully developed conditions (hydrodynamic and thermal);
(6) negligible axial heat conduction in the substrate and the fluid; and
(7) averaged convective heat transfer coefficient h for the cross section.

In the approximate analyses considered, this set of assumptions is progressively relaxed.

Model 1 – 1D resistance analysis

In addition to making assumptions 1 – 7 above, the temperature is assumed uniform over any cross section in the simplest of the models.

For fully developed flow under a constant heat flux, the temperature profile within the microchannel in the axial direction is shown in Figure 4. The three components of the heat transfer process are:

$$q_{cond} = k_s A_s \frac{T_{w,o} - T_{b,o}}{t} \tag{12}$$

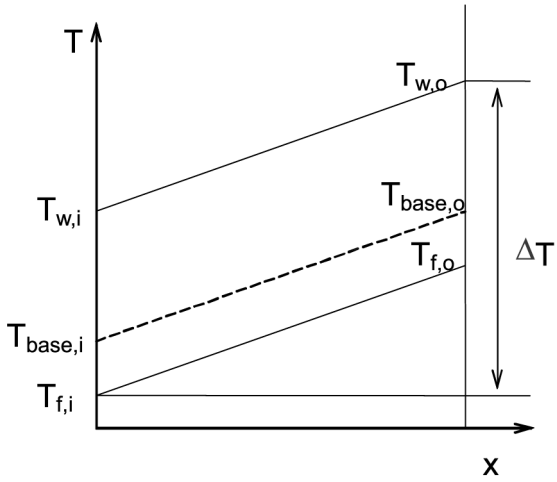

Figure 4.
Temperature profile in a microchannel heat sink

$$q_{\text{conv}} = hA_{\text{f}}(T_{\text{b}} - \overline{T}_{\text{f}}) \tag{13}$$

$$q_{\text{cal}} = \rho QC_p(T_{\text{f,o}} - T_{\text{f,i}}) \tag{14}$$

The overall thermal resistance can thus be divided into three components:

$$\text{R}_{\text{o}} = \frac{\Delta T_{\max}}{q''(LW)} = \frac{1}{q''(LW)}[(T_{\text{w,o}} - T_{\text{f,i}})] = R_{\text{cond}} + R_{\text{conv}} + R_{\text{cal}} \tag{15}$$

in which the three resistances may be determined as follows:

(1) Conductive thermal resistance

$$R_{\text{cond}} = \frac{t}{k_{\text{s}}(LW)} \tag{16}$$

(2) Convective thermal resistance

$$R_{\text{conv}} = \frac{1}{nhL(2\eta_{\text{f}}H_{\text{c}} + w_{\text{c}})} \tag{17}$$

with fin efficiency $\eta_{\text{f}} = \tanh(mH_{\text{c}})/mH_{\text{c}}$.

(3) Caloric thermal resistance:

$$R_{\text{cal}} = \frac{1}{\rho_{\text{f}}OC_p} \tag{18}$$

Model 2 – fin analysis

In this model, assumptions 1-7 mentioned above are adopted, and the fluid temperature profile is considered one-dimensional (averaged over *y-z* cross section), $T_{\text{f}} = T_{\text{f}}(x)$. The temperature distribution in the solid fin is then:

$$\frac{d^2T}{dy^2} = \frac{2h}{k_s w_w}(T - T_f(x)) \tag{19}$$

with boundary conditions:

$$-k_s \left.\frac{dT}{dy}\right|_{y=0} = \frac{2\eta_f \alpha}{2\eta_f \alpha + 1}\frac{w_c + w_w}{w_w} q'' \tag{20}$$

$$\left.\frac{dT}{dy}\right|_{y=H_c} = 0 \tag{21}$$

It follows that

$$T(x,y) = T_f(x) + \frac{1}{m}\frac{q''}{k_s}\frac{2\eta_f \alpha}{2\eta_f \alpha + 1}\frac{w_c + w_w}{w_w}\frac{\cosh\{m(H_c - y)\}}{\sinh(mH_c)} \tag{22}$$

where $m = (2h/k_s w_w)^{1/2}$.

The fluid temperature $T_f(x)$ can be obtained from an energy balance:

$$\dot{m} C_p \frac{dT_f(x)}{dx} = q''(w_c + w_w) \tag{23}$$

with $T_f(x = 0) = T_0$. The bulk fluid temperature is then:

$$T_f(x) = T_0 + \frac{q''(w_c + w_w)}{\rho_f C_p u_m H_c w_c} x \tag{24}$$

and equation (22) can be rewritten as:

$$T(x,y) = T_0 + \frac{1}{m}\frac{q''}{k_s}\frac{2\eta_f \alpha}{2\eta_f \alpha + 1}\frac{w_c + w_w}{w_w}\frac{\cosh\{m(H_c - y)\}}{\sinh(mH_c)} + \frac{q''(w_c + w_w)}{\rho_f C_p u_m H_c w_c} x \tag{25}$$

The thermal resistance is thus:

$$\begin{aligned} R &= \frac{\Delta T}{q''(LW)} = \frac{T(L,0) - T_0}{q''(LW)} \\ &= \frac{1}{m}\frac{1}{k_s}\frac{2\eta_f \alpha}{2\eta_f \alpha + 1}\frac{w_c + w_w}{w_w}\frac{\cosh(mH_c)}{\sinh(mH_c)}\frac{1}{(LW)} + \frac{(w_c + w_w)}{\rho_f C_p u_m H_c w_c}\frac{1}{W} \end{aligned} \tag{26}$$

Model 3 – fin-fluid coupled approach I

Following the same line of reasoning as in the fin analysis (model 2) and adopting assumptions 1-7 mentioned above, but averaging the fluid temperature only in the z direction (Samalam, 1989), the energy equation in the fin can be written as:

$$\frac{\partial^2 T}{\partial y^2} = \frac{2h}{k_s w_w}(T - T_f(x,y)) \tag{27}$$

with

$$-k_s \left.\frac{\partial T}{\partial y}\right|_{y=0} = \frac{2\eta_f \alpha}{2\eta_f \alpha + 1} \frac{w_c + w_w}{w_w} q'' = J \tag{28}$$

$$\left.\frac{\partial T}{\partial y}\right|_{y=H_c} = 0 \tag{29}$$

The energy balance in the fluid is represented by:

$$\rho_f C_p u_m w_c \frac{\partial T_f}{\partial x} = 2h(T - T_f(x,y)) \tag{30}$$

and it is assumed that $T_f(x = 0, y) = 0$. Substituting $h = Nuk_f/D_h$ into equation (30) yields:

$$\frac{1}{2}\rho_f C_p u_m w_c D_h \frac{\partial T_f}{\partial x} + k_f \mathrm{Nu} T_f = k_f \mathrm{Nu} T \tag{31}$$

Defining $X = x/a$ and $Y = y/a$ where $a = \rho_f C_p u_m w_c D_h / 2k_f \mathrm{Nu}$, the solution to equation (31) can be written as:

$$T_f(X, Y) = \int_0^X T(X', Y) e^{-(X - X')} \, dX' \tag{32}$$

Hence, equation (27) can then be transformed to:

$$\frac{\partial^2 T(X, Y)}{\partial Y^2} = \beta \left\{ T(X, Y) - \int_0^X T(X', Y) e^{-(X - X')} \, dX' \right\} \tag{33}$$

in which

$$\beta = \frac{a^2}{\lambda^2} \tag{34}$$

$$\lambda^2 = \frac{k_s w_w D_h}{2k_f \mathrm{Nu}} \tag{35}$$

Solving equation (33) by Laplace transforms,

$$\frac{\partial^2 f(Y, s)}{\partial Y^2} = \gamma f \quad \left(\gamma = \frac{\beta_s}{s + 1}\right) \tag{36}$$

The boundary conditions in equations (28) and (29) become:

$$-k_s \left.\frac{\partial f}{\partial Y}\right|_{Y=0} = \frac{Ja}{s} \tag{37}$$

$$-k_s \left.\frac{\partial f}{\partial Y}\right|_{Y=\tilde{H}_c} = 0 \tag{38}$$

where $\tilde{H}_c = H_c/a$, and J is defined in equation (28). The solution to this system of equations is:

$$f(s) = \frac{Ja}{k_s s\sqrt{\gamma}} \frac{\cosh\left(\sqrt{\gamma}(Y - \tilde{H}_c)\right)}{\sinh\left(\sqrt{\gamma}\tilde{H}_c\right)} \tag{39}$$

The inverse Laplace transform yields the temperature:

$$\begin{aligned} T(X, Y) &= L^{-1}[f(s, Y)] \\ &= \frac{Ja}{k_s \tilde{H}_c \beta} \left\{ (1 + X) + \frac{\beta}{2}(Y - \tilde{H}_c)^2 - \frac{\beta \tilde{H}_c^2}{6} \right. \\ &\quad \left. + 2\sum_{n=1}^{\infty} (-1)^n \frac{(s_n + 1)^2}{s_n} \cos\left[\frac{n\pi(Y - \tilde{H}_c)}{\tilde{H}_c}\right] e^{s_n X} \right\} \end{aligned} \tag{40}$$

in which

$$s_n = \frac{-n^2\pi^2/\tilde{H}_c^2}{\beta + n^2\pi^2/\tilde{H}_c^2}.$$

This is a rapidly converging infinite series for which the first three terms adequately represent the thermal resistance:

$$R = \frac{\Delta T}{q''(LW)} = \frac{T(L, 0) - T_0}{q''(LW)} = \frac{Ja}{k_s \tilde{H}_c \beta} \left[(1 + L/a) + \frac{1}{3}\beta \tilde{H}_c^2 \right] \frac{1}{(LW)} \tag{41}$$

Model 4 – fin-fluid coupled approach II

In this model, assumptions 1-7 mentioned above are again adopted, except that axial conduction in the fin is not neglected (Sabry, 2001). The governing equations in the solid fin and liquid, respectively, are therefore:

$$\nabla^2 T(x, y, z) = 0 \tag{42}$$

$$\nabla \cdot (\rho_f C_p \vec{V} T_f(x, y, z)) = k_f \nabla^2 T_f(x, y, z) \tag{43}$$

At the fin-fluid interface, the condition is:

$$-k_s \frac{\partial T_s}{\partial z} = -k_f \frac{\partial T_f}{\partial z} = h(T_i - \overline{T}_f) \tag{44}$$

in which the averaged local fluid temperature is:

$$\overline{T}_f(x) = \int_0^{w_c/2} v T_f \, dz / (u_m w_c/2) \tag{45}$$

with

$$u_{\mathrm{m}} = \int_0^{w_{\mathrm{c}}/2} v \, \mathrm{d}z / w_{\mathrm{c}}/2.$$

Along with equation (28), the following boundary conditions apply:

$$\left.\frac{\partial T}{\partial y}\right|_{y=H_{\mathrm{c}}} = \left.\frac{\partial T}{\partial x}\right|_{x=0} = \left.\frac{\partial T}{\partial x}\right|_{x=L} = \left.\frac{\partial T}{\partial z}\right|_{z=-\frac{w_{\mathrm{w}}}{2}} = \left.\frac{\partial T_{\mathrm{f}}}{\partial z}\right|_{z=\frac{w_{\mathrm{c}}}{2}} = 0 \tag{46}$$

Integrating equation (42) over z from $-w_{\mathrm{w}}/2$ to 0, the fin temperature varies as:

$$\frac{w_{\mathrm{w}}}{2}\left(\frac{\partial^2}{\partial x^2} + \frac{\partial^2}{\partial y^2}\right)\overline{T} + \left.\frac{\partial \overline{T}}{\partial z}\right|_{-\frac{w_{\mathrm{w}}}{2}}^{0} = 0 \tag{47}$$

in which

$$\overline{T} = \int_{-\frac{w_{\mathrm{w}}}{2}}^{0} T \, \mathrm{d}z / (w_{\mathrm{w}}/2).$$

Combining equations (44) and (46),

$$k_{\mathrm{s}} \frac{w_{\mathrm{w}}}{2}\left(\frac{\partial^2}{\partial x^2} + \frac{\partial^2}{\partial y^2}\right)\overline{T} - h(T_i - \overline{T}_{\mathrm{f}}) = 0 \tag{48}$$

Assuming $T_i = \overline{T}$, since $B_i = h(w_{\mathrm{w}}/2)/k_{\mathrm{s}} \ll 1$, equation (48) becomes:

$$k_{\mathrm{s}} \frac{w_{\mathrm{w}}}{2}\left(\frac{\partial^2}{\partial x^2} + \frac{\partial^2}{\partial y^2}\right)\overline{T} - h(\overline{T} - \overline{T}_{\mathrm{f}}) = 0 \tag{49}$$

If the axial conduction term $\partial^2 \overline{T}/\partial x^2$ is neglected, equation (49) would reduce to equation (27).

Since fully developed conditions are assumed and axial conduction in the fluid is neglected, equation (43) may be integrated over z from 0 to $w_{\mathrm{c}}/2$ to yield:

$$\frac{\partial}{\partial x}\int_0^{w_{\mathrm{c}}/2} u T_{\mathrm{f}} \, \mathrm{d}z = \frac{k_{\mathrm{f}}}{\rho_{\mathrm{f}} C_p} \left.\frac{\partial T_{\mathrm{f}}}{\partial z}\right|_0^{\frac{w_{\mathrm{c}}}{2}} \tag{50}$$

Using the boundary condition in equation (44), this reduces to

$$u_{\mathrm{m}} \frac{w_{\mathrm{c}}}{2} \frac{\partial}{\partial x}\overline{T}_{\mathrm{f}} + \frac{1}{\rho_{\mathrm{f}} C_p} h(\overline{T}_{\mathrm{f}} - \overline{T}) = 0 \tag{51}$$

The following dimensionless variables are introduced:

$$X = x/L, \quad Y = y/H_{\mathrm{c}}, \quad \text{and} \quad T = \frac{\overline{T} - T_0}{\Delta T_{\mathrm{c}}} \tag{52}$$

in which

$$\Delta T_c = \frac{2\eta_f \alpha}{2\eta_f \alpha + 1} \frac{(w_c + w_w)/2}{hH_c} q'' \tag{53}$$

The system of equations above can be cast in dimensionless terms:

$$\left(A^2 \frac{\partial^2}{\partial X^2} + \frac{\partial^2}{\partial Y^2} \right) T - (mH_c)^2 (T - T_f) = 0 \tag{54}$$

$$\frac{\partial T_f}{\partial X} + S(T_f - T) = 0 \tag{55}$$

$$\left. \frac{\partial T}{\partial Y} \right|_{Y=0} = -(mH_c)^2 \tag{56}$$

$$\left. \frac{\partial T_s}{\partial X} \right|_{X=1} = \left. \frac{\partial T_s}{\partial Y} \right|_{Y=0} = \left. \frac{\partial T_s}{\partial Y} \right|_{Y=1} = 0 \tag{57}$$

$$T_f|_{X=0} = 0 \tag{58}$$

where $A = H_c/L$ and the modified Stanton number (Sabry, 2001) is given by:

$$S = hL \Big/ \left(\rho_f C_p u_m \frac{w_c}{2} \right).$$

Employing similar techniques as adopted for model 3, the fin temperature is obtained as:

$$T(X, Y) = mH_c \frac{\cosh(mH_c(1 - Y))}{\sinh(mH_c)} + \sum_{n=0}^{\infty} \cos(n\pi Y) f_n(X) \tag{59}$$

in which the first term in the infinite series provides results of acceptable accuracy (<5 percent deviation from the complete series):

$$f_0(X) = SX + \sum_{i=1}^{2} \left(\frac{C_{0i}}{w_{0i}} \right) e^{w_{0i}X} + C_{03} \tag{60}$$

with

$$w_{01} = -\frac{S}{2} + \sqrt{\left(\frac{S}{2} \right)^2 + \left(\frac{mH_c}{A} \right)^2}$$

$$w_{02} = -\frac{S}{2} - \sqrt{\left(\frac{S}{2} \right)^2 + \left(\frac{mH_c}{A} \right)^2}$$

$$C_{01} = -S \frac{(e^{w_{02}} - 1)}{(e^{w_{02}} - e^{w_{01}})}$$

$$C_{02} = -S\frac{(e^{w_{01}} - 1)}{(e^{w_{02}} - e^{w_{01}})}$$

$$C_{03} = \left(\frac{SA}{mH_c}\right)^2$$

The thermal resistance is thus obtained as:

$$R = \frac{\Delta T}{q''(LW)} = \frac{T(1,0) - T_0}{q''(LW)}\Delta T_c$$
$$= \frac{2\eta_f\alpha}{2\eta_f\alpha + 1}\frac{w_c + w_w}{2hH_c}\left[mH_c\frac{\cosh(mH_c)}{\sinh(mH_c)} + S + \sum_{i=1}^{2}\left(\frac{C_{0i}}{w0_i}\right)e^{w_{0i}} + C_{03}\right]\frac{1}{(LW)} \quad (61)$$

In most practical cases, $(mH_c/A) \gg S/2$, and equation (61) reduces to:

$$R = \frac{2\eta_f\alpha}{2\eta_f\alpha + 1}\frac{w_c + w_w}{2hH_c}\left[mH_c\frac{\cosh(mH_c)}{\sinh(mH_c)} + S + \left(\frac{SA}{mH_c}\right)^2\right]\frac{1}{(LW)} \quad (62)$$

Model 5 – porous medium approach

The convective heat transfer process in microchannels can also be treated as being similar to that in a fluid-saturated porous medium, with the extended Darcy equation used for fluid flow and a volume-averaged two-equation model used for heat transfer, as demonstrated in Vafai and Tien (1981).

Following the analysis of Kim and Kim (1999), a two-equation model can be employed to obtain the volume-averaged properties over a representative elementary volume for the solid region and the fluid region separately. The momentum equation and boundary conditions are:

$$-\frac{d}{dx}\langle p\rangle_f + \mu_f\frac{d^2}{dy^2}\langle u\rangle_f - \frac{\mu_f}{K}\varepsilon\langle u\rangle_f = 0 \quad (63)$$

$$\langle u\rangle_f = 0 \quad \text{at } y = 0, H_c \quad (64)$$

where $\langle u\rangle_f$ is the volume-averaged velocity, $\varepsilon = w_c/(w_c + w_w)$ is the porosity, and $K = \varepsilon w_c^2/12$ is the permeability. Equations (63) and (64) may be written as:

$$U = Da\frac{d^2U}{dY^2} - P \quad (65)$$

$$U = 0 \quad \text{at} \quad Y = 0, 1 \quad (66)$$

using the dimensionless parameters:

$$U = \frac{\langle u\rangle_f}{u_m}, \quad Da = \frac{K}{\varepsilon H^2} = \frac{1}{12\alpha_s^2}, \quad Y = \frac{y}{H}, \quad P = \frac{K}{\varepsilon\mu_f u_m}\frac{d\langle p\rangle_f}{dx}.$$

The solution to the momentum equation is then:

$$U = P\left\{\cosh\left(\sqrt{\frac{1}{Da}}Y\right) + \frac{1-\cosh\left(\sqrt{\frac{1}{Da}}\right)}{\sinh\left(\sqrt{\frac{1}{Da}}\right)}\sinh\left(\sqrt{\frac{1}{Da}}Y\right) - 1\right\} \tag{67}$$

The volume-averaged energy equations for the fin and fluid, respectively, are:

$$k_{se}\frac{\partial^2\langle T\rangle}{\partial y^2} = ha(\langle T\rangle - \langle T\rangle_f) \tag{68}$$

$$\varepsilon\rho_f C_p\langle u\rangle_f\frac{\partial\langle T\rangle_f}{\partial x} = ha(\langle T\rangle - \langle T\rangle_f) + k_{fe}\frac{\partial^2\langle T\rangle_f}{\partial y^2} \tag{69}$$

with boundary conditions

$$\langle T\rangle = \langle T\rangle_f = T_w \quad \text{at } y = 0 \tag{70}$$

$$\frac{\partial\langle T\rangle}{\partial y} = \frac{\partial\langle T\rangle_f}{\partial y} = 0 \quad \text{at } y = H_c \tag{71}$$

where a is the wetted area per unit volume, h the local heat transfer coefficient defined as the ratio of the interfacial heat flux to the solid-fluid temperature difference, and k_{se} and k_{fe} the effective conductivities of the solid and fluid, defined as $k_{se} = (1-\varepsilon)k_s, k_{fe} = \varepsilon k_f$.

For fully developed flow under constant heat flux, it is known that

$$\frac{\partial\langle T\rangle_f}{\partial x} = \frac{\partial\langle T\rangle}{\partial x} = \frac{dT_w}{dx} = \text{constant} \tag{72}$$

and

$$q'' = \varepsilon\rho_f C_p u_m H\frac{\partial\langle T\rangle_f}{\partial x} \tag{73}$$

The energy equations (68) and (69) and boundary conditions can thus be written in dimensionless form as:

$$\frac{d^2\theta}{dY^2} = D(\theta - \theta_f) \tag{74}$$

$$U = D(\theta - \theta_f) + C\frac{d^2\theta_f}{dY^2} \tag{75}$$

with

$$\theta = \theta_f = 0 \quad \text{at } Y = 0 \tag{76}$$

$$\frac{d\theta}{dY} = \frac{d\theta_f}{dY} = 0 \quad \text{at } Y = 1 \tag{77}$$

in which

$$C = \frac{\varepsilon k_f}{(1-\varepsilon)k_s}, \quad D = \frac{haH^2}{(1-\varepsilon)k_s}, \quad \theta = \frac{\langle T\rangle - T_w}{\frac{q''H}{(1-\varepsilon)k_s}}, \quad \theta_f = \frac{\langle T\rangle_f - T_w}{\frac{q''H}{(1-\varepsilon)k_s}}.$$

Substituting the solution obtained for velocity, equations (74) and (75) can be solved to give:

$$\theta_f = \frac{P}{1+C}\left[-\frac{1}{2}Y^2 + C_1 Y + C_2 - C_3\cosh\left(\sqrt{\frac{D(1+C)}{C}}Y\right) - C_4\sinh\left(\sqrt{\frac{D(1+C)}{C}}Y\right) + C_5\left\{\cosh\left(\sqrt{\frac{1}{Da}}Y\right) + \frac{1-\cosh\left(\sqrt{\frac{1}{Da}}\right)}{\sinh\left(\sqrt{\frac{1}{Da}}\right)}\sinh\left(\sqrt{\frac{1}{Da}}Y\right)\right\}\right] \tag{78}$$

$$\theta = P\left[Da\left\{\cosh\left(\sqrt{\frac{1}{Da}}Y\right) + \frac{1-\cosh\left(\sqrt{\frac{1}{Da}}\right)}{\sinh\left(\sqrt{\frac{1}{Da}}\right)}\sinh\left(\sqrt{\frac{1}{Da}}Y\right)\right\} - \frac{1}{2}Y^2 + C_1 Y - Da\right] - C\theta_f \tag{79}$$

where

$$N_1 = D(1+C)\sqrt{\frac{1}{Da}\left\{1-\cosh\left(\sqrt{\frac{1}{Da}}\right)\right\}}$$

$$N_2 = \frac{C}{Da}\sqrt{\frac{D(1+C)}{C}}\sinh\left(\sqrt{\frac{1}{Da}}\right)\sinh\left(\sqrt{\frac{D(1+C)}{C}}\right)$$

$$C_1 = 1 - \frac{\sqrt{Da}\left(\cosh\left(\sqrt{\frac{1}{Da}}\right)-1\right)}{\sinh\left(\sqrt{\frac{1}{Da}}\right)}$$

$$C_2 = -Da + \frac{1}{D(1+C)}$$

$$C_3 = \frac{C}{DaD(1+C)D_1}$$

$$C_4 = \frac{N_1 + N_2}{D(1+C)\sqrt{\frac{D(1+C)}{C}}\cosh\left(\sqrt{\frac{D(1+C)}{C}}\,Y\right)\sinh\left(\sqrt{\frac{1}{Da}}\right)D_1}$$

$$C_5 = Da - \frac{1}{D_1}$$

Finally, the thermal resistance can be obtained as:

$$R = \frac{12K}{\rho_f C_p w_c^3 \alpha W \varepsilon^2 u_m} - \frac{\theta_{f,b} H_c}{(1-\varepsilon) k_s L W} \tag{80}$$

in which $\theta_{f,b}$ is the bulk mean fluid temperature, defined as:

$$\theta_{f,b} = \int_0^1 U\theta_f \, dY \Big/ \int_0^1 U \, dy$$

Key features of the five approximate models discussed above, including the assumptions, governing equations and resistance formulae developed, are summarized in Table II.

Assessment of the approximate models

For the microchannel parameters listed in Table I, thermal resistances were computed with Fluent as well as from the five approximate models. The results are shown in Table III. It can be seen that all the approximate models would provide acceptable predictions for the thermal resistance of the microchannel heat sink, with the maximum deviation being 7.8 percent. Models 2-5 are more complex to apply than model 1, and involve the solution of the differential governing equations. In spite of its simplicity, model 1 appears to adequately represent the physics of the heat transfer problem, and is recommended for use in the design and optimization of practical microchannel heat sinks.

It may be noted that in model 2, the fluid temperature is considered to be only a function of the x-coordinate, and the fin temperature is solved in a truly 1D manner. The thermal resistance expression from model 2 is therefore identical to that from model 1. Also, in models 3 and 4, since 2D temperature fields are considered in both the fin and fluid, the new terms $H_c/(3nk_s w_w L)$ and $(1/(\rho_f C_p Q)^2)(nk_s H_c w_w/L)$ appear, in addition to the other terms in the simpler models 1 and 2. The difference between models 3 and 4 is that the axial conduction term appears explicitly in the fin equation of model 4, while it is neglected in model 3.

In the calculations above, expressions for Nusselt number, Nu, and the friction constant, fRe, are needed for computing the convective heat transfer coefficient, h, and the average velocity, u_m in the microchannel. In all the five approximate models discussed above, the flow is assumed to be thermally and hydrodynamically fully developed. Hence the following relations are used in terms of microchannel aspect ratios (Incropera and DeWitt, 1996; Shah and London, 1978):

$$\mathrm{Nu}_{fd} = 8.235(1 - 1.883\alpha + 3.767\alpha^2 - 5.814\alpha^3 + 5.361\alpha^4 - 2\alpha^5) \tag{81}$$

$$(f\mathrm{Re})_{fd} = 96(1 - 1.3553/\alpha + 1.9467/\alpha^2 - 1.7012/\alpha^3 + 0.9564/\alpha^4 - 0.2537/\alpha^5) \tag{82}$$

Table II.
Summary of approximate analytical models

Model	Axial conduction Fin	Axial conduction Fluid	Temperature Fin	Temperature Fluid	Governing equations	Thermal resistance (R)
1	1D	1D	×	×	Not used	$\frac{1}{nhL(2\eta_f H_c + w_c)} + \frac{1}{\rho_f Q C_p}$ (88)
2	2D	1D	×	×	$\frac{d^2T}{dy^2} - \frac{hP}{k_s A_c}(T - T_f(x)) = 0$ $\dot{m}C_p \frac{dT_f(x)}{dx} = q \cdot (w_c + w_w)$	$\frac{1}{nhL(2\eta_f H_c + w_c)} + \frac{1}{\rho_f C_p Q}$ (89)
3	2D	2D	×	×	$k_s \frac{\partial^2 T}{\partial y^2} = \frac{2h}{w_w}(T - T_f(x,y))$ $\rho_f C_p u_m w_c \frac{\partial T_f}{\partial x} = 2h(T - T_f(x,y))$	$\frac{Ja}{k_s \tilde{H}_c \beta}\left[(1 + L/a) + \frac{1}{3}\beta \tilde{H}_c^2\right]\frac{1}{(LW)}$ (90)
4	2D	2D	√	×	$\nabla^2 T(x,y,z) = 0$ $\nabla \cdot (\vec{V} T_f(x,y,z)) = \alpha_f \nabla^2 T_f(x,y,z)$	$\frac{2\eta_f \alpha}{2\eta_f \alpha + 1}\left[\frac{1}{2nhH_c \eta_f L} + \frac{1}{\rho_f C_p Q} + \frac{1}{(\rho_f C_p Q)^2}\frac{nk_s H_c w_w}{L}\right]$ (91)
5	1D	1D	×	×	$-\frac{d}{dx}\langle p \rangle_f + \mu_f \frac{d^2}{dy^2}\langle u \rangle_f - \frac{\mu_f}{k}\varepsilon \langle u \rangle_f = 0$ $k_{se}\frac{\partial^2 \langle T \rangle}{\partial y^2} = ha(\langle T \rangle - \langle T \rangle_f)$ $\varepsilon \rho_f C_p \langle u \rangle_f \frac{\partial \langle T \rangle_f}{\partial x} = ha(\langle T \rangle - \langle T \rangle_f) + k_{fe}\frac{\partial^2 \langle T \rangle_f}{\partial y^2}$	$\frac{12K}{\rho_f C_p w_c^3 \alpha W \varepsilon^2 u_m} - \frac{\theta_{f,h} H_c}{(1-\varepsilon)k_s LW}$ (92)

Notes: × – not considered; and √ – considered

However, the fully developed assumption is not always valid, especially for microchannels with the larger hydraulic diameters and short lengths. With hydrodynamic and thermal lengths defined as $L^+ = L/(D_h \mathrm{Re})$ and $L^* = L/(D_h \mathrm{RePr})$, the following relations (Samalam, 1989; Harms *et al.*, 1999) could be employed instead of equations (81) and (82):

$$\mathrm{Nu} = 3.35(L^*)^{-0.13}\alpha^{0.12}\mathrm{Pr}^{-0.038}, \quad 0.013 \le L^* < 0.1 \tag{83}$$

$$\mathrm{Nu} = 1.87(L^*)^{-0.30}\alpha^{0.056}\mathrm{Pr}^{-0.036}, \quad 0.0005 \le L^* < 0.013 \tag{84}$$

$$f_{\mathrm{app}}\mathrm{Re} = \left[\left\{\frac{3.2}{(L^+)^{0.57}}\right\}^2 + (f\mathrm{Re})_{fd}^2\right]^{1/2}, \quad L^+ < 0.05 \tag{85}$$

In the present calculations, $L/D_h \approx 100$ with moderate Reynolds numbers, so that the hydrodynamically fully developed condition is satisfied. For the working fluid in this study (water, Prandtl number ~ 5.8), Nusselt numbers calculated from equations (81) and (83) are listed in Table IV. The deviation between the two sets of results is within 6 percent, and therefore, the assumption of thermally fully developed conditions is acceptable. In general, developing thermal effects should be carefully considered before fully developed conditions are assumed.

Optimization

The optimization of microchannel heat sink design can be motivated using the thermal resistance approach in model 1. As indicated in equation (18), R_{cal} is inversely proportional to the mass flow rate. When the pressure head along the microchannel length is prescribed as the constraint, R_{cal} will decrease as w_c increases when H_c reaches the maximum allowable value. However, the convective heat transfer coefficient h will increase when D_h decreases, leading to a reduction in R_{conv}, as shown by equation (17). The heat transfer from the substrate through the fins will also be enhanced if the fin efficiency increases, which requires a larger fin

Table III. Overall thermal resistances

Thermal resistance (°C/W)	Case 1	Case 2	Case 3
$R_{\mathrm{o,num}}$	0.115	0.114	0.093
$R_{\mathrm{o,model\ 1}}$	0.112	0.112	0.091
$R_{\mathrm{o,model\ 2}}$	0.112	0.112	0.091
$R_{\mathrm{o,model\ 3}}$	0.106	0.106	0.087
$R_{\mathrm{o,model\ 4}}$	0.106	0.106	0.087
$R_{\mathrm{o,model\ 5}}$	0.115	0.106	0.089

Table IV. Nusselt numbers

	Case 1	Case 2	Case 3
Nu_{fd}	5.97	5.81	6.06
Nu	5.60	5.55	5.85

thickness w_w. However, the increase in w_w will reduce the number of microchannel/fin pairs in a heat sink for a prescribed heat sink size. Due to these competing factors, there exists an optimal microchannel dimension that minimizes the overall thermal resistance.

In order to optimize the thermal performance of a microchannel heat sink, the following variables must be specified from implementation constraints:

(1) thermal conductivity of the bulk material used to construct the heat sink (k_s);

(2) overall dimension of the heat sink (L and W from the size of the chip, H_c and t from fabrication and structural considerations);

(3) properties of the coolant (ρ_f, μ, k_f, C_p); and

(4) allowable pressure head (ΔP).

To illustrate the procedure, the example considered uses water as the working fluid to cool a chip with $L = W = 1$ cm and a given pressure head of $\Delta P = 60$ kPa. The heat load is 100 W/cm^2. The microchannel heat sink is to be made of silicon with $t = 100\,\mu$m and $H_c = 400\,\mu$m. The fluid properties are evaluated at 27 °C. The optimization process involves finding the optimal microchannel geometry (channel width w_c, fin thickness w_w and aspect ratio $\alpha = H_c/w_c$) that will minimize thermal resistance.

Solutions to the following equations would yield the optimum:

$$\frac{\partial R}{\partial w_c} = 0 \tag{86}$$

$$\frac{\partial R}{\partial w_w} = 0 \tag{87}$$

In this work, the optimization computations were performed using the commercial solver MATLAB (The Math Works, Inc., 2001). The optimized results derived from the five approximate models are listed in Table V. The optimal thermal resistance values reported from the five models agree to the within 10 percent. It may also be noted that the minimum thermal resistance is always attained at the largest allowable aspect ratio. In practical designs, the aspect ratio would be determined by the limits on the microchannel depth and the substrate thickness.

Conclusions

Five approximate analytical models for predicting the convective heat transfer in microchannel heat sinks are presented and compared. Closed-form solutions from these models are compared to full CFD simulation and experimental results, and the efficacy

Model	w_c (μm)	w_w (μm)	α	R_o (°C/W)
1	64	18	6.25	0.0965
2	65	19	6.15	0.0965
3	65	24	6.15	0.0973
4	61	16	6.56	0.0907
5	64	27	6.25	0.1072

Table V.
Optimal dimensions

of the different models assessed. Optimization procedures are discussed for minimizing the thermal resistance of the heat sinks. The results obtained demonstrate that the models developed offer sufficiently accurate predictions for practical designs, while at the same time being quite straightforward to use.

References

Fedorov, A.G. and Viskanta, R. (2000), "Three-dimensional conjugate heat transfer in the microchannel heat sink for electronic packaging", *International Journal of Heat and Mass Transfer*, Vol. 43, pp. 399-415.

Fluent Inc. (1998), *Fluent User's Guide*, Lebanon, New Hampshire.

Harms, T.M., Kazmierczak, M.J. and Gerner, F.M. (1999), "Developing convective heat transfer in deep rectangular microchannels", *International Journal of Heat and Fluid Flow*, Vol. 20, pp. 149-57.

Incropera, F.P. and DeWitt, D.P. (1996), *Fundamentals of Heat and Mass Transfer*, Wiley, New York, NY.

Kim, S.J. and Kim, D. (1999), "Forced convection in microstructure for electronic equipment cooling", *Journal of Heat Transfer*, Vol. 121, pp. 639-45.

The MathWorks, Inc. (2001), Matlab, Version 6.1, Natwick, MA.

Ryu, J.H., Choi, D.H. and Kim, S.J. (2002), "Numerical optimization of the thermal performance of a microchannel heat sink", *International Journal of Heat and Mass Transfer*, Vol. 45, pp. 2823-7.

Sabry, M-N. (2001), "Transverse temperature gradient effect on fin efficiency for microchannel design", *Journal of Electronic Packaging*, Vol. 123, pp. 344-50.

Samalam, V.K. (1989), "Convective heat transfer in microchannels", *Journal of Electronic Materials*, Vol. 18, pp. 6111-7.

Shah, R.K. and London, A.L. (1978), "Laminar flow forced convection in ducts", *Advances in Heat Transfer, Supplement 1*, Academic Press, London.

Sobhan, C.B. and Garimella, S.V. (2001), "A comparative analysis of studies on heat transfer and fluid flow in microchannels", *Microscale Thermophysical Engineering*, Vol. 5, pp. 293-311.

Toh, K.C., Chen, X.Y. and Chai, J.C. (2002), "Numerical computation of fluid flow and heat transfer in microchannels", *International Journal of Heat and Mass Transfer*, Vol. 45, pp. 5133-41.

Tuckerman, D.B. and Pease, R.F. (1981), "High-performance heat sinking for VLSI", *IEEE Electronic Devices Letters EDL-2*, pp. 126-9.

Vafai, K. and Tien, C.L. (1981), "Boundary and inertia effects on flow and heat transfer in porous media", *International Journal of Heat and Mass Transfer*, Vol. 24, pp. 195-203.

Weisberg, A. and Bau, H.H. (1992), "Analysis of microchannels for integrated cooling", *International Journal of Heat and Mass Transfer*, Vol. 35, pp. 2465-74.

Zhao, C.Y. and Lu, T.J. (2002), "Analysis of microchannel heat sinks for electronics cooling", *International Journal of Heat and Mass Transfer*, Vol. 45, pp. 4857-69.

Further reading

Tien, C.L. and Kuo, S.M. (1987), "Analysis of forced convection in microstructures for electronic system cooling", *Proc. Int. Symp. Cooling Tech. for Electronic Equipment*, Honolulu, HI, pp. 217-26.